

## Multiphase carbon mineralization for the reactive separation of CO<sub>2</sub> and directed synthesis of H<sub>2</sub>

Greeshma Gadikota 

**Abstract** | There is a need to capture, convert and store CO<sub>2</sub> by atom-efficient and energy-efficient pathways that use as few process configurations as possible. This need has motivated studies into multiphase reaction chemistries and this Review describes two such approaches in the context of carbon mineralization. The first approach uses aqueous alkaline solutions containing amine nucleophiles that capture CO<sub>2</sub> and eventually convert it into calcium and magnesium carbonates, thereby regenerating the nucleophiles. Gas–liquid–solid and liquid–solid configurations of these reactions are explored. The second approach combines silicates such as CaSiO<sub>3</sub> or Mg<sub>2</sub>SiO<sub>4</sub> with CO and H<sub>2</sub>O from the water–gas shift reaction to give H<sub>2</sub> and calcium or magnesium carbonates. Coupling carbonate formation to the water–gas shift reaction shifts the latter equilibrium to afford more H<sub>2</sub> as part of a single-step catalytic approach to carbon mineralization. These pathways exploit the vast abundance of alkaline resources, including naturally occurring silicates and alkaline industrial residues. However, simple stoichiometries belie the complex, multiphase nature of the reactions, predictive control of which presents a scientific opportunity and challenge. This Review describes this multiphase chemistry and the knowledge gaps that need to be addressed to achieve ‘step-change’ advancements in the reactive separation of CO<sub>2</sub> by carbon mineralization.

A major societal challenge is to meet our rising energy and resource needs while lowering CO<sub>2</sub> emissions and their detrimental environmental impacts. This challenge calls for advancing novel reactive-separation pathways for the integrated and accelerated capture, conversion and storage of CO<sub>2</sub>. A particularly prominent approach is to convert anthropogenic CO<sub>2</sub> into naturally occurring inorganic solid carbonates by thermodynamically downhill reactions. On the field scale, efforts to elucidate the natural uptake of CO<sub>2</sub> in Mg<sub>2</sub>SiO<sub>4</sub> deposits<sup>1–3</sup> and mine tailings<sup>4</sup> to yield magnesium carbonates have afforded crucial insights into the role of multiphase reaction pathways. The key reactions involved include the partitioning of CO<sub>2</sub> from the gas to the liquid phase, dissolution of the alkaline Mg/Ca compounds and formation of water-insoluble calcium or magnesium carbonates. Which of these reactions is rate-limiting depends on temperature *T*, partial pressure *p*(CO<sub>2</sub>), pH, ionic strength, the composition of contacting fluids and the accessible reactive surface area. In the context of subsurface CO<sub>2</sub> storage, the accelerated conversion of mobile CO<sub>2</sub> into calcium or magnesium carbonates has shown promise for lowering the costs associated with tracking the fate and transport of mobile CO<sub>2</sub>.

Field-scale injections of CO<sub>2</sub> into reactive basalt formations in Iceland<sup>5</sup> and in the State of Washington in the United States<sup>6,7</sup> have shown that CO<sub>2</sub> can be trapped as calcium or magnesium carbonates. Mimicking these gas–liquid–solid reaction pathways in a laboratory (‘geomimicry’) shows that temperatures at or above 100 °C and *p*(CO<sub>2</sub>) >50 atm lead to >90% conversion of the silicates CaSiO<sub>3</sub> or Mg<sub>2</sub>SiO<sub>4</sub> to calcium or magnesium carbonates<sup>8–13</sup>. While elevated temperatures favour the dissolution kinetics of silicates<sup>14</sup> and the precipitation of calcium and magnesium carbonates<sup>15,16</sup>, they also lead to lower CO<sub>2</sub> solubility. The dissolution of CO<sub>2</sub> in an aqueous phase can, however, be driven by using high partial pressures. A challenge associated with the reaction network is that, when pH <4, alkaline earth salts can dissolve and release Ca<sup>2+</sup> or Mg<sup>2+</sup> ions into an aqueous phase, but carbonate formation is most favoured when pH >8. It is possible to dissolve basic solids and precipitate calcium carbonate and/or magnesium carbonate in tandem by using pH buffers and carbonate carriers such as NaHCO<sub>3</sub> (REFS<sup>8–13</sup>). Thus, high-purity, pressurized CO<sub>2</sub> can be converted into and stored as calcium and magnesium carbonates, but using a separate unit operation for capturing and compressing CO<sub>2</sub> is not practical.

School of Civil and  
Environmental Engineering,  
Cornell University, Ithaca,  
NY, USA.

e-mail: [gg464@cornell.edu](mailto:gg464@cornell.edu)

<https://doi.org/10.1038/s41570-019-0158-3>

**Table 1 | Representative reactions in the directed synthesis of H<sub>2</sub> with integrated carbon mineralization**

Entry	Reaction	$\Delta H$ (kJ mol <sup>-1</sup> )
1	$2\text{CO} + 2\text{H}_2\text{O} \rightarrow 2\text{CO}_2 + 2\text{H}_2$	-82.4
2	$\text{Mg}_2\text{SiO}_4 + 2\text{H}_2\text{O} \rightarrow 2\text{Mg}(\text{OH})_2 + \text{SiO}_2$	-99.7
3	$2\text{Mg}(\text{OH})_2 \rightarrow 2\text{MgO} + 2\text{H}_2\text{O}$	162.4
4	$2\text{MgO} + 2\text{CO}_2 \rightarrow 2\text{MgCO}_3$	-235.6
5 (1 + 2 + 3 + 4)	$\text{Mg}_2\text{SiO}_4 + 2\text{CO} + 2\text{H}_2\text{O} \rightarrow 2\text{MgCO}_3 + \text{SiO}_2 + 2\text{H}_2$	-255.3
6	$\text{CO} + \text{H}_2\text{O} \rightarrow \text{CO}_2 + \text{H}_2$	-41.2
7	$\text{CaSiO}_3 + \text{H}_2\text{O} \rightarrow \text{Ca}(\text{OH})_2 + \text{SiO}_2$	-24.3
8	$\text{Ca}(\text{OH})_2 \rightarrow \text{CaO} + \text{H}_2\text{O}$	108.4
9	$\text{CaO} + \text{CO}_2 \rightarrow \text{CaCO}_3$	-178.4
10 (6 + 7 + 8 + 9)	$\text{CaSiO}_3 + \text{CO} + \text{H}_2\text{O} \rightarrow \text{CaCO}_3 + \text{SiO}_2 + \text{H}_2$	-135.5

Such experiments raise the larger scientific question of how we might design multiphase reaction pathways to capture, convert and store CO<sub>2</sub> in a single carbon-mineralization process. Conceptualizing chemical pathways to address this question yields two approaches. In the first approach, the low aqueous solubility of CO<sub>2</sub> is overcome by using a solution in which one or more nucleophilic components has a high affinity for CO<sub>2</sub> at room temperature. The resulting CO<sub>2</sub>-bearing solution is basic and also contains Ca<sup>2+</sup> or Mg<sup>2+</sup> ions, such that calcium and magnesium carbonates precipitate. Thus, the CO<sub>2</sub>-binding molecules are regenerated chemically instead of thermally, whereby the CO<sub>2</sub> adduct is heated to isolate CO<sub>2</sub>. The aim of coupling these reactions is to use CO<sub>2</sub> from flue gas streams (1 atm) to produce calcium and magnesium carbonates at *T* < 100 °C. In the second approach, reactive separation of CO<sub>2</sub> by carbon mineralization is used for the directed synthesis of clean energy carriers, such as H<sub>2</sub>. Specifically, CO and H<sub>2</sub>O (steam) undergo the water-gas shift reaction (WGSR) to give H<sub>2</sub> and CO<sub>2</sub>, with the latter going on to react with

CaSiO<sub>3</sub> or Mg<sub>2</sub>SiO<sub>4</sub> to give calcium and magnesium carbonates. This means of removing CO<sub>2</sub> from the WGSR means that the equilibrium shifts to afford more H<sub>2</sub> (TABLE 1), which is ideally produced at temperatures in the range 150–250 °C in a single catalytic carbon mineralization pathway — an alternative to the two-step catalytic approach in which one stage requires 310–450 °C and the other 200–250 °C<sup>17</sup>. Several minerals and rocks have been explored for carbon mineralization (TABLE 2).

This Review describes the multiphase chemical transformations underlying the two above approaches and identifies the scientific knowledge gaps associated with chemistry at solid interfaces. Indeed, the extents of carbon mineralization are often unpredictable, and it is difficult to direct the synthesis of calcium or magnesium carbonates with structural and morphological specificity and characterize chemo-morphological coupling in multiphase reaction environments. Addressing these challenges will allow us to develop technologies that are preferable to the conventional approach of independently developing separation media for CO<sub>2</sub> capture, designing catalytic pathways for CO<sub>2</sub> conversion and optimizing CO<sub>2</sub> storage in subsurface environments. According to the National Academies of Sciences, Engineering, and Medicine (2019)<sup>12</sup>, carbon mineralization of Mg-containing or Ca-containing ultramafic (basic, O<sup>2-</sup>/OH<sup>-</sup>-rich materials such as serpentine, (Mg,Fe)<sub>3</sub>Si<sub>2</sub>O<sub>5</sub>(OH)<sub>4</sub>) tailings, alkaline industrial residues, construction and demolition waste, municipal solid waste and naturally occurring minerals such as peridotite, all together, can offset up to 30 Gt CO<sub>2</sub> per year. These assessments are based on conventional carbon-mineralization approaches, the costs of which must be lowered to enable large-scale implementation. This is what motivates the exploration of novel reactive-separation pathways of CO<sub>2</sub> that use alkaline residues and naturally occurring minerals.

### Alkaline-amine looping in carbon mineralization

I now detail the rational design of multiphase chemical reaction pathways involved in the first CO<sub>2</sub> processing approach, whereby aqueous nucleophiles — amines being the most prominent — bind CO<sub>2</sub> en route to the formation of carbonates in basic solution. Described first are the early studies that led to these amine technologies.

**Early research motivating the design of integrated reaction pathways.** The desirability of an integrated chemical pathway — a single reaction environment for the direct capture, conversion and storage of CO<sub>2</sub> as calcium or magnesium carbonates — led to the exploration of chemically regenerable solvents containing amine or amino-acid groups that bind CO<sub>2</sub>. Further, several efforts were dedicated to accelerating the dissolution of CO<sub>2</sub>, alkaline-bearing minerals and industrial residues, and their precipitation into calcium or magnesium carbonates. These studies were undertaken independently of each other, such that the stages were individually improved without considering their possible roles in a larger, coupled reaction pathway. For example, biomimetic pathways using enzymes such as carbonic anhydrase were targeted at accelerating CO<sub>2</sub> hydration to produce HCO<sub>3</sub><sup>-</sup> and CO<sub>3</sub><sup>2-</sup>

**Table 2 | Names and representative chemical compositions of minerals and rocks of interest for carbon mineralization**

Name	Representative chemical composition
Anorthite	CaAl <sub>2</sub> Si <sub>2</sub> O <sub>8</sub>
Augite	(Ca,Na)(Mg,Fe,Al,Ti)(Si,Al) <sub>2</sub> O <sub>6</sub>
Calcite, aragonite, vaterite	CaCO <sub>3</sub>
Forsterite	Mg <sub>2</sub> SiO <sub>4</sub>
Hydromagnesite	Mg <sub>5</sub> (CO <sub>3</sub> ) <sub>4</sub> (OH) <sub>2</sub> ·4H <sub>2</sub> O
Lizardite and antigorite (serpentine analogues)	(Mg,Fe) <sub>3</sub> Si <sub>2</sub> O <sub>5</sub> (OH) <sub>4</sub>
Magnesite	MgCO <sub>3</sub>
Nesquehonite	MgCO <sub>3</sub> ·3H <sub>2</sub> O
Olivine	(Mg,Fe) <sub>2</sub> SiO <sub>4</sub>
Wollastonite	CaSiO <sub>3</sub>
Anorthosite	Mixture comprising anorthite and olivine
Basalt	Mixture comprising plagioclase feldspar (anorthite, NaAlSi <sub>3</sub> O <sub>8</sub> (albite), XY(Si,Al) <sub>2</sub> O <sub>6</sub> (pyroxene; X = Ca, Na, Fe, Mg; Y = Fe <sup>III</sup> , Mg, Co, Mn, Sc, Ti, V, Fe <sup>II</sup> , Cr, Al) and olivine)

in the aqueous phase<sup>18,19</sup>. Separately, ligands such as citrate, acetate and ethylenediaminetetraacetate were explored to enhance chelation and aqueous extraction of  $\text{Ca}^{2+}$  and  $\text{Mg}^{2+}$  from solids, particularly from siliceous minerals<sup>20</sup>. When Ca-containing and Mg-containing silicates are the sources of alkalinity, the formation of  $\text{SiO}_2$  passivates the silicate surface and limits the rate at which  $\text{Ca}^{2+}$  and  $\text{Mg}^{2+}$  can be extracted into the aqueous phase<sup>21–23</sup>. One approach to overcome this problem is to include reagents such as catechol<sup>24</sup> or Zr–organic frameworks<sup>25</sup> to cleave Si–O bonds and release Si oxyanions into the aqueous environment. What remains is to optimize the rate of carbonate precipitation, and studies towards this have proposed the use of seed crystals to lower the free-energy barrier to nucleation<sup>26,27</sup>. Thus, each sequential reaction step in low-temperature carbon mineralization can be tuned by adding reagents and making the necessary pH adjustments. However, at the time, there was limited understanding of the energetics associated with using these reagents and the regeneration efficiency. Accordingly, there has been a lot of research conducted on chemically regenerable amine-bearing or amino-acid-bearing solvents for integrated  $\text{CO}_2$  capture, conversion and storage.

#### ***$\text{CO}_2$ capture with aqueous amines or amino acids.***

Aqueous solutions of amines can efficiently capture  $\text{CO}_2$  at temperatures in the range 40–60 °C (REF.<sup>28</sup>). These  $\text{CO}_2$ -loaded solutions are regenerated at 120–140 °C to liberate high-purity  $\text{CO}_2$  (REF.<sup>28</sup>). The widespread use of these solutions and continued interest in novel solvents and mixtures is motivated by their fast kinetics and ease of regeneration<sup>29,30</sup>. The  $\text{CO}_2$  capture mechanism, capacity and regeneration efficiency depend on the structure of the amine. For example, in terms of theoretical capacity, two primary or secondary amine molecules are needed to capture one  $\text{CO}_2$  molecule in the form of a carbamate (with some ending up as  $\text{HCO}_3^-$ )<sup>31</sup>. Tertiary amines and sterically bulky secondary amines act as Brønsted rather than Lewis bases, and only one molecule of amine is stoichiometrically required to capture  $\text{CO}_2$  and afford  $\text{HCO}_3^-$  and  $\text{CO}_3^{2-}$  hydrolysis products<sup>31</sup>. Relative to primary and secondary amines, tertiary and cyclic amines are more chemically and thermally stable<sup>31</sup>.

The environmental problem with using amine-bearing solvents for  $\text{CO}_2$  capture is that their thermal and chemical degradation affords harmful products, such as nitrosamines, nitramines and ammonia<sup>31–38</sup>. Indeed, many amines are not 100% regenerable from

their carbamate/bicarbonate forms, and their degradation products corrode carbon-steel infrastructure for  $\text{CO}_2$  capture<sup>39–43</sup>. This led some to study amine mixtures to optimize  $\text{CO}_2$  capture and mineralization<sup>44,45</sup> or, preferably, the use of environmentally benign and stable alternatives such as amino-acid salts<sup>46–60</sup> (FIG. 1). Indeed, potassium and sodium glycinate have faster  $\text{CO}_2$ -binding kinetics, lower binding energies, lower vapour pressures, greater thermal stabilities and superior  $\text{O}_2$  resistances relative to ethanolamine derivatives<sup>51,53,54</sup>. Glycine reacts with  $\text{CO}_2$  to generate the corresponding carbamic acid, which is deprotonated by a second equivalent of glycinate to produce the corresponding carbamate and zwitterionic glycine<sup>55</sup>. The carbamate undergoes hydrolysis to afford glycinate and  $\text{HCO}_3^-$  ions<sup>55</sup>. Not all amino-acid salts are suitable for carbon mineralization. For example, potassium sarcosinate ((methylamino)acetate) precipitates from aqueous solution on capturing  $\text{CO}_2$  (REFS<sup>56–60</sup>) and is unsuitable as a  $\text{CO}_2$  absorbent because the precipitate cannot quickly combine with the  $\text{M}^{2+}$  ions and base to give calcium or magnesium carbonates. Indeed, when using absorbents in an alkaline aqueous phase to capture  $\text{CO}_2$  and release it by chemical regeneration, the objective is to precipitate only calcium or magnesium carbonates while maintaining the  $\text{CO}_2$ -binding nucleophile in the aqueous phase. Aside from capacity for  $\text{CO}_2$  and solubility of adducts, several other criteria need to be considered when evaluating amine bases for carbon mineralization. Desirable attributes for integrated  $\text{CO}_2$  capture, conversion and storage by carbon mineralization include the retention of flowability without enhanced viscosity on  $\text{CO}_2$  capture and regeneration, retention of activity through multiple cycles of carbon mineralization, negligible generation of non-carbonate precipitates as end products and ease of chemical regeneration by carbon mineralization.

#### ***Integrated pathways for $\text{CO}_2$ absorption and carbonate crystallization.***

Let us first consider  $\text{CO}_2$  absorption in the absence of an amine base. Carbon mineralization in natural systems often occurs over timescales of several years, and efforts to engineer this to occur over a few hours can go two ways. In one method, introducing  $\text{CO}_2$  (139 atm) into aqueous NaCl (1.0 M) and  $\text{NaHCO}_3$  (0.64 M) with 15 wt%  $\text{Mg}_2\text{SiO}_4$  at temperatures up to 185 °C yielded 85% conversion in a single 3-h step<sup>9</sup>. As described above, elevated  $p(\text{CO}_2)$  aids dissolution into the aqueous phase, while elevated  $T$  favours the kinetics of  $\text{Mg}_2\text{SiO}_4$  dissolution<sup>61,62</sup> and  $\text{MgCO}_3$  precipitation<sup>15,16</sup>. Analogously, when  $\text{CO}_2$  (40 atm) is added to a mixture at 100 °C that contains  $\text{CaSiO}_3$  instead of  $\text{Mg}_2\text{SiO}_4$ , one observes complete conversion into  $\text{CaCO}_3$  over the same period<sup>8</sup>. Life-cycle assessments show that, after accounting for energy requirements, substantial amounts of  $\text{CO}_2$  are sequestered using these pathways<sup>63</sup>. The second approach involves dissolving the Ca-bearing and Mg-bearing minerals to extract  $\text{Ca}^{2+}$  and  $\text{Mg}^{2+}$  into the aqueous phase using strong acids, after which the pH must be raised to above 9 before bubbling  $\text{CO}_2$  in to precipitate calcium or magnesium carbonates<sup>64–66</sup>. This pH-swing process is chemically intensive but does convert  $\text{CaSiO}_3$  or  $\text{Mg}_2\text{SiO}_4$  into high-purity carbonates and  $\text{SiO}_2$ .

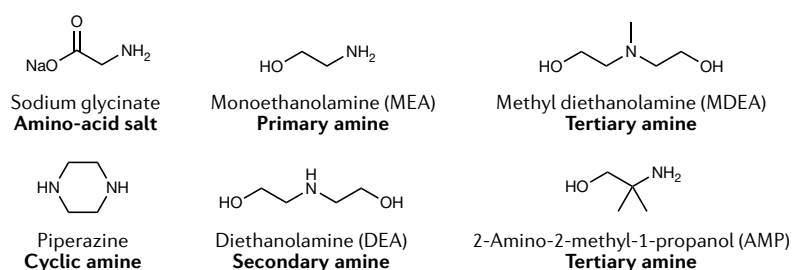


Fig. 1 | **Amines used to capture  $\text{CO}_2$  in aqueous solution.** Figure adapted with permission from REF.<sup>70</sup>, Royal Society of Chemistry.

The search for less energetically or chemically intensive pathways for carbon mineralization motivated the exploration of aqueous solutions of amine sorbents<sup>46–49,67</sup>. For example, a recent study has shown CO<sub>2</sub>-loaded monoethanolamine (MEA; FIG. 1) to be effective for the carbonate-assisted solidification of CaSiO<sub>3</sub> particles, thus enabling cementation for construction-related applications<sup>46</sup>. However, the recycling efficiency of the aqueous amine solution was not quantified<sup>46</sup>. After this study, it was found that aqueous solutions of CO<sub>2</sub>-loaded amines such as MEA (FIG. 1), diethanolamine (DEA), piperazine (PZ), 2-amino-2-methyl-1-propanol (AMP) and methyl diethanolamine (MDEA) enable complete

conversion of CaO into CaCO<sub>3</sub> at 40 °C. PZ absorbed the most CO<sub>2</sub> and exhibited the greatest regeneration efficiency on a molar basis of amines — the percentage of CO<sub>2</sub>-loaded absorbent converted back to the base on mineralization<sup>47</sup>. The regeneration energy of PZ is lower because it acts by coupling absorption and mineralization, which contrasts the conventional thermal regeneration of amines<sup>68</sup>. Similarly, CaCl<sub>2</sub> solutions undergo complete conversion into CaCO<sub>3</sub> when combined with CO<sub>2</sub>-loaded MEA, AMP or MDEA<sup>49</sup>. MEA, DEA and MDEA favoured the formation of calcite (rhombohedral CaCO<sub>3</sub>), while using AMP gave calcite, as well as the hexagonal polymorph vaterite<sup>49</sup>.

The carbon-mineralization studies described above used CO<sub>2</sub>-loaded amines in liquid–solid environments<sup>47</sup>, as opposed to more realistic gas–liquid–solid environments featuring CO<sub>2</sub>-containing flue gas. Recent studies using CO<sub>2</sub> gas, an amine-bearing solution and a Ca-bearing or Mg-bearing alkaline substrate show that one can directly use the gas and still have rapid carbon mineralization with regeneration of the amine (FIG. 2). For example, under CO<sub>2</sub> (1 atm), one can vary the identity of the alkaline solid (15 wt% CaO<sup>69</sup>, CaSiO<sub>3</sub> (REF.<sup>69</sup>) or MgO<sup>70</sup> in H<sub>2</sub>O) and the MEA concentration (0–50 wt%) to study the effects on carbonate formation. In the case of CaO and CaSiO<sub>3</sub>, the presence of MEA greatly accelerates mineralization<sup>69</sup> (FIG. 3a). Aqueous suspensions of MgO with 50 wt% MEA afforded a gel-like phase under CO<sub>2</sub> that limited mass transfer and lowered the extent of carbon mineralization<sup>70</sup>. The composition of the gel phase was not anticipated and mechanisms by which these phases form are not well understood. The formation of gels as a potential rate-limiting step needs more detailed investigation. Each alkaline solid undergoes single-step carbon mineralization most readily at 50 °C (FIG. 3b) — a moderate temperature amenable to CO<sub>2</sub> dissolution. Another parameter of amine-catalysed carbon mineralization is the enthalpy of the reaction, and further studies should explore this parameter to inform a more rational selection of amine. Nevertheless, these results show that CO<sub>2</sub> solvation, dissolution of the alkaline solids and carbonate precipitation can be coupled in a single gas–liquid–solid reaction environment, presenting the possibility of an integrated pathway that can be coupled to point sources of CO<sub>2</sub> or to an existing CO<sub>2</sub>-capture plant that utilizes amine-bearing solvents.

**The nature of the alkaline solid affects which carbonate phase forms.** Capturing and converting CO<sub>2</sub> in flue gas is optimal when the alkaline Ca<sup>2+</sup> or Mg<sup>2+</sup> solution affords CaCO<sub>3</sub> or MgCO<sub>3</sub> instead of metastable or hydrated species such as MgCO<sub>3</sub>·xH<sub>2</sub>O. When using basic aqueous CaCl<sub>2</sub> as the precursor, aqueous solutions of amines such as MEA, DEA and MDEA yield pure calcite crystals, while AMP affords calcite and vaterite at 40 °C (REF.<sup>49</sup>). The co-formation of stable and metastable carbonate phases is evident when CO<sub>2</sub> contacts MgO or CaO suspended in aqueous MEA. For example, MgO often affords metastable MgCO<sub>3</sub>·3H<sub>2</sub>O (nesquehonite) and MgCO<sub>3</sub>·5H<sub>2</sub>O (lansfordite) (FIG. 4a), whereas CaO can afford the thermodynamic product calcite but also metastable aragonite and vaterite<sup>69</sup> (FIG. 4b).

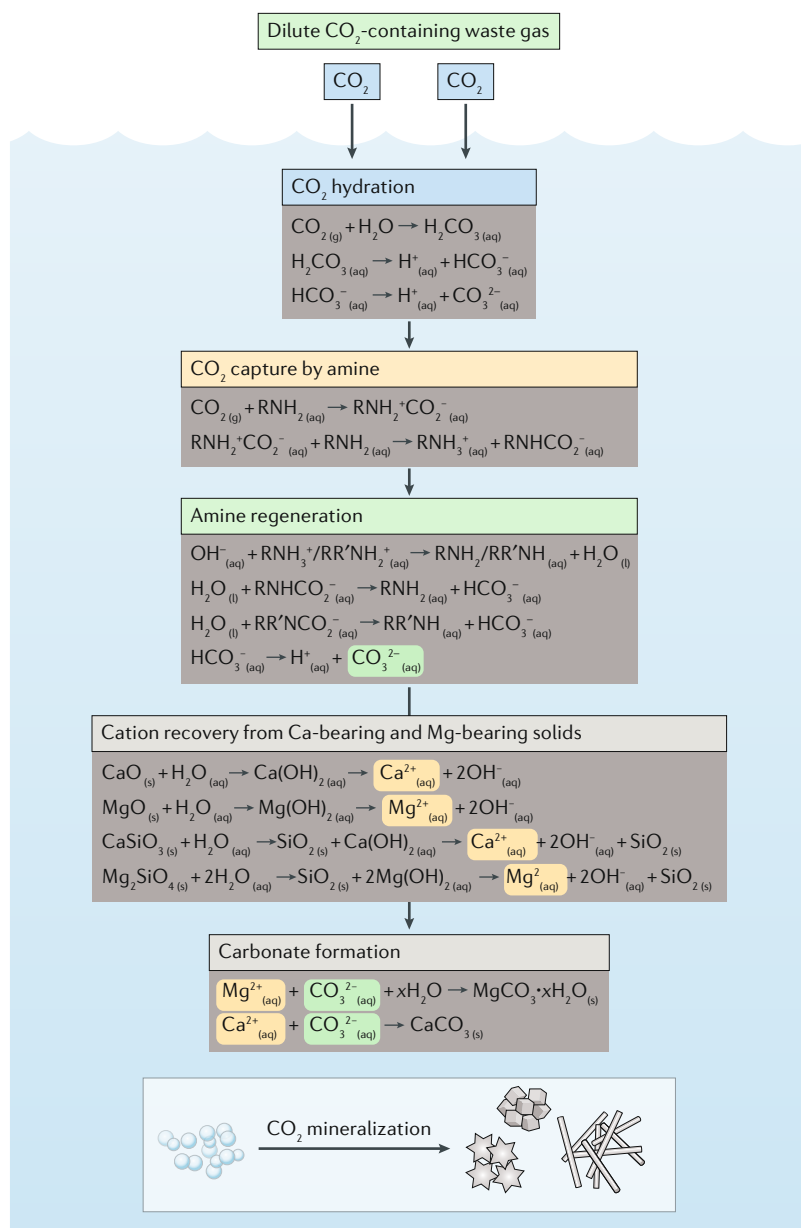


**Fig. 2 | The aqueous alkaline-amine-looping approach for CO<sub>2</sub> mineralization.** In principle, all reactions are reversible. CO<sub>2</sub> first undergoes partitioning from the gas to the aqueous phase, in which it can be captured by an amine to give a carbamate (in the case of primary amines). The carbamate can readily be converted back into the amine and the CO<sub>3</sub><sup>2-</sup> ions that form combine with dissolved Ca<sup>2+</sup> and/or Mg<sup>2+</sup> to give CaCO<sub>3</sub> and MgCO<sub>3</sub>·xH<sub>2</sub>O<sup>69,70</sup>.



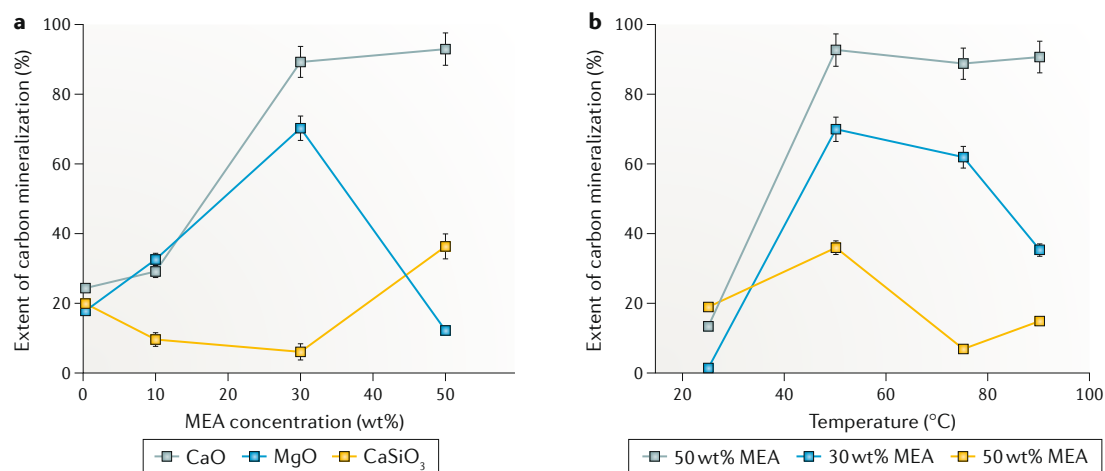


**Fig. 3 | Carbon mineralization by aqueous alkaline-amine looping is affected by the solid precursor, temperature and amine concentration.** **a** | Effect of monoethanolamine (MEA) concentration on the extent of carbon mineralization ( $T = 50\text{ }^{\circ}\text{C}$ , 15 wt% solid precursor,  $p(\text{CO}_2) = 1\text{ atm}$ , 3 h stirring at 300 rpm). **b** | Effect of temperature on the extent of carbon mineralization (50 wt% MEA for CaO, 30 wt% MEA for MgO and 50 wt% MEA for CaSiO<sub>3</sub>, 15 wt% solid precursor,  $p(\text{CO}_2) = 1\text{ atm}$ , 3 h stirring at 300 rpm)<sup>69,70</sup>. Error bars represent standard deviations based on triplicate analyses. Figure adapted with permission from REF.<sup>69</sup>, American Chemical Society.

When one makes carbonates from earth-abundant silicate minerals such as CaSiO<sub>3</sub> and Mg<sub>2</sub>SiO<sub>4</sub> or alkaline industrial residues such as coal fly ash, steel slag and cement kiln dust, it is important to elucidate how the different solid interfaces compete as sites for carbonate crystallization. For example, carbonate growth on MgCO<sub>3</sub> surfaces is more favourable than on Mg(OH)<sub>2</sub>, a result attributed to high self-adhesion and the large misfit between the two phases<sup>71</sup>. When comparing and contrasting the precipitation behaviour of calcium or magnesium carbonates, the role of the hydration shell is an important consideration. Mg<sup>2+</sup> has a higher charge density and more stable hydration spheres than Ca<sup>2+</sup>, so calcite can precipitate six orders of magnitude more quickly than magnesite (MgCO<sub>3</sub>) at 25 °C (REF.<sup>72,73</sup>). Exploring how solid interfaces influence the formation of carbonate phases will allow us to control the chemistry and morphologies of the carbonate products.

### H<sub>2</sub> synthesis coupled to carbon mineralization

The rationale for exploring H<sub>2</sub> production coupled to separation of co-generated CO<sub>2</sub> lies in our growing interest to produce carbon-neutral or carbon-negative energy carriers as alternatives to fossil-derived hydrocarbon resources<sup>74,75</sup>. Scalable H<sub>2</sub> production first involves gasification, whereby organic feedstocks such as carbonaceous fuels or non-recyclable plastics are reacted under O<sub>2</sub> or steam to produce CO, H<sub>2</sub> and CO<sub>2</sub> (REF.<sup>76</sup>). The CO produced is further reformed in steam to produce CO<sub>2</sub> and H<sub>2</sub> through the WGS:  $\text{CO} + \text{H}_2\text{O} \rightleftharpoons \text{CO}_2 + \text{H}_2$  ( $\Delta H = -41.2\text{ kJ mol}^{-1}$ ). This reaction is favoured at low temperatures but suffers from slow kinetics. Thus, conventional processes involve two catalytic systems to rapidly obtain high conversion: one operating between 310 °C and 450 °C and another between 200 °C and 250 °C (REF.<sup>17,77</sup>), with the respective pressures being 10 atm and 20 atm (REF.<sup>78</sup>). As mentioned above, removing CO<sub>2</sub> by carbon mineralization will shift the equilibrium

to the products, affording more H<sub>2</sub> and enabling a previously two-stage catalytic step to be performed in a single stage<sup>79</sup>. The following sections describe the feasibility of such a setup.

**Adaptive chemical pathways for H<sub>2</sub> production from carbonaceous sources.** The WGS is a highly versatile pathway for converting carbonaceous fuels that range from coal and natural gas to biomass and non-recyclable plastics<sup>17,80,81</sup>. As an alternative to this gas–solid reaction, a single aqueous alkaline catalytic environment has been proposed to aid the conversion of CO and steam into CO<sub>2</sub> and H<sub>2</sub> (REFS<sup>82,83</sup>), because high pressures and excess H<sub>2</sub>O drive the WGS to near completion. The benefit of excess H<sub>2</sub>O has led to extensive studies of an aqueous chemical loop in which: (i) CO<sub>3</sub><sup>2-</sup> reacts to form OH<sup>-</sup> and CO<sub>2</sub>, (ii) OH<sup>-</sup> reacts with CO to produce HCO<sub>2</sub><sup>-</sup>, (iii) HCO<sub>2</sub><sup>-</sup> disproportionates to CO<sub>3</sub><sup>2-</sup> and H<sub>2</sub>CO, after which (iv) H<sub>2</sub>CO decomposes to yield H<sub>2</sub>. The rate-limiting step is the disproportionation of HCO<sub>2</sub><sup>-</sup> (REF.<sup>83</sup>), a problem that can be addressed using catalysis. For example, aqueous HCO<sub>2</sub>K converts into H<sub>2</sub> over catalysts such as 5–10% Pd on activated carbon<sup>84</sup>.

It is desirable to limit the number of stages in the conventional gas–solid WGS and facilitate the removal of CO<sub>2</sub>. This has led to the proposal of a sorption-enhanced water-gas shift reaction, in which an alkaline sorbent is used to capture CO<sub>2</sub> (REFS<sup>58,85–95</sup>). For example, CaO sorbents are activated by steam to give Ca(OH)<sub>2</sub> materials that are highly effective in capturing CO<sub>2</sub> and producing high-purity CaCO<sub>3</sub> in the temperature range 300–600 °C (REF.<sup>85</sup>). Mg(OH)<sub>2</sub> has also been proposed as a sorbent<sup>96</sup>, but its gas–solid reaction with CO<sub>2</sub> to produce MgCO<sub>3</sub> is mass-transfer-limited<sup>96</sup>. This can be addressed using slurry carbonation of Mg(OH)<sub>2</sub> (REF.<sup>97</sup>), with the required CO<sub>2</sub> coming from the near-complete conversion of CO and steam over catalysts such as Pt<sup>79</sup>. Despite these demonstrated successes of using Ca(OH)<sub>2</sub> and Mg(OH)<sub>2</sub>

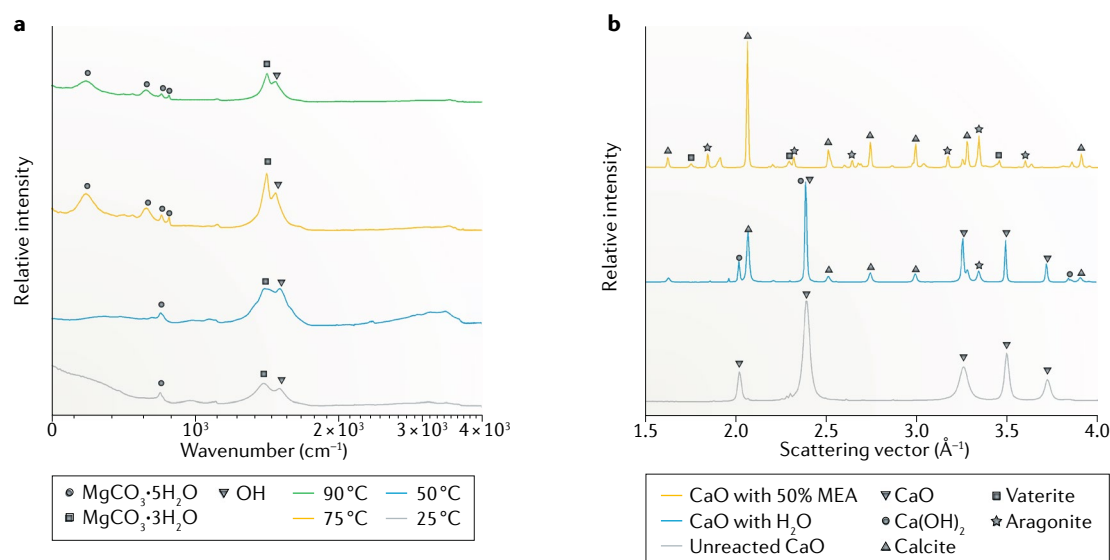


**Fig. 4 | Polymorphism in calcium and magnesium carbonate products of carbon mineralization.** **a** | Attenuated total reflectance Fourier transform infrared spectroscopy reveals how MgO converts into metastable hydrated phases such as  $\text{MgCO}_3 \cdot 3\text{H}_2\text{O}$  (nesquehonite) and  $\text{MgCO}_3 \cdot 5\text{H}_2\text{O}$  (lansfordite) in aqueous monoethanolamine (MEA)-catalysed mineralization (30 wt% MEA,  $T = 50^\circ\text{C}$ ,  $p(\text{CO}_2) = 1 \text{ atm}$ , 3 h stirring at  $300 \pm 5 \text{ rpm}$ )<sup>70</sup>. **b** | Wide-angle X-ray scattering patterns of CaO transforming into metastable aragonite and vaterite, along with calcite, proceeds in  $\text{H}_2\text{O}$  and even more quickly in 50 wt% aqueous MEA<sup>69</sup>. Part **a** adapted with permission from REF.<sup>70</sup>, Royal Society of Chemistry. Part **b** adapted with permission from REF.<sup>69</sup>, American Chemical Society.

in directing the synthesis of  $\text{H}_2$ , substantial  $\text{CO}_2$  emissions are associated with synthesizing these hydroxides. As an alternative, the use of earth-abundant minerals such Ca-bearing and Mg-bearing silicates needs to be explored. I now describe this approach, which is

potentially attractive because it effects carbon mineralization under conditions similar to those that favour the WGRS.

#### Geomimicry of carbon mineralization for $\text{CO}_2$ storage.

Converting and storing  $\text{CO}_2$  as calcium or magnesium carbonates is a potentially permanent and thermodynamically downhill carbon-mineralization route. Several efforts have been directed towards mimicking and potentially accelerating these natural carbon-mineralization processes<sup>16,19,38,46,66,98–100</sup>. These studies have suggested that the timescales of the conversion of  $\text{Mg}_2\text{SiO}_4$  into  $\text{MgCO}_3$ , which are on the order of several years, can be lowered to a few hours (FIG. 5). Indeed, under similar temperatures and pressures,  $\text{Mg}_2\text{SiO}_4$  (forsterite) and  $\text{CaSiO}_3$  (wollastonite) are much more reactive than aluminosilicate minerals such as anorthite and rocks such as basalt<sup>101</sup> (FIG. 5). For example, the extent of the carbon mineralization in  $(\text{Mg,Fe})_2\text{SiO}_4$  (olivine) and wollastonite can be greater than 80%, making these materials useful sorbents for the WGRS.

#### Directed synthesis of $\text{H}_2$ and carbonates from silicates.

Several factors affect the directed synthesis of  $\text{H}_2$  and calcium and magnesium carbonates from  $\text{CaSiO}_3$  or  $\text{Mg}_2\text{SiO}_4$ . Forsterite and wollastonite undergo carbon mineralization best at temperatures above  $90^\circ\text{C}$  (REF.<sup>101</sup>) (FIG. 5), because the kinetics of mineral dissolution become faster<sup>61,62</sup> and the solubility of the product carbonates<sup>15,16</sup> becomes lower with increasing temperature. These studies suggest that relatively high conversions of  $\text{CaSiO}_3$  and  $\text{Mg}_2\text{SiO}_4$  into their respective carbonates can be achieved at conditions that correspond to the low-temperature WGRS. The thermal stability of magnesite

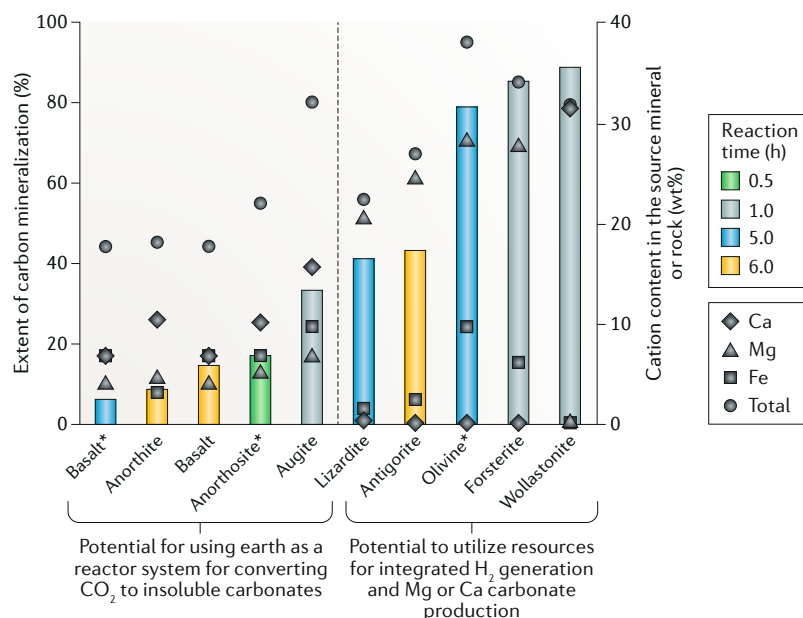


**Fig. 5 | Comparison of the reactivity of Ca-bearing and Mg-bearing silicate and aluminosilicate minerals and rocks.** The extents of the mineralization are reflected in the bars and cation contents denoted by shapes ( $T = 185^\circ\text{C}$ ,  $p(\text{CO}_2) = 150 \text{ atm}$ , in aqueous  $\text{NaCl}$  (1.0 M) and  $\text{NaHCO}_3$  (0.64 M))<sup>8,98,101</sup>. Asterisks indicate the studies performed by the present author. All others were reported in publications by Gerdemann and co-workers.

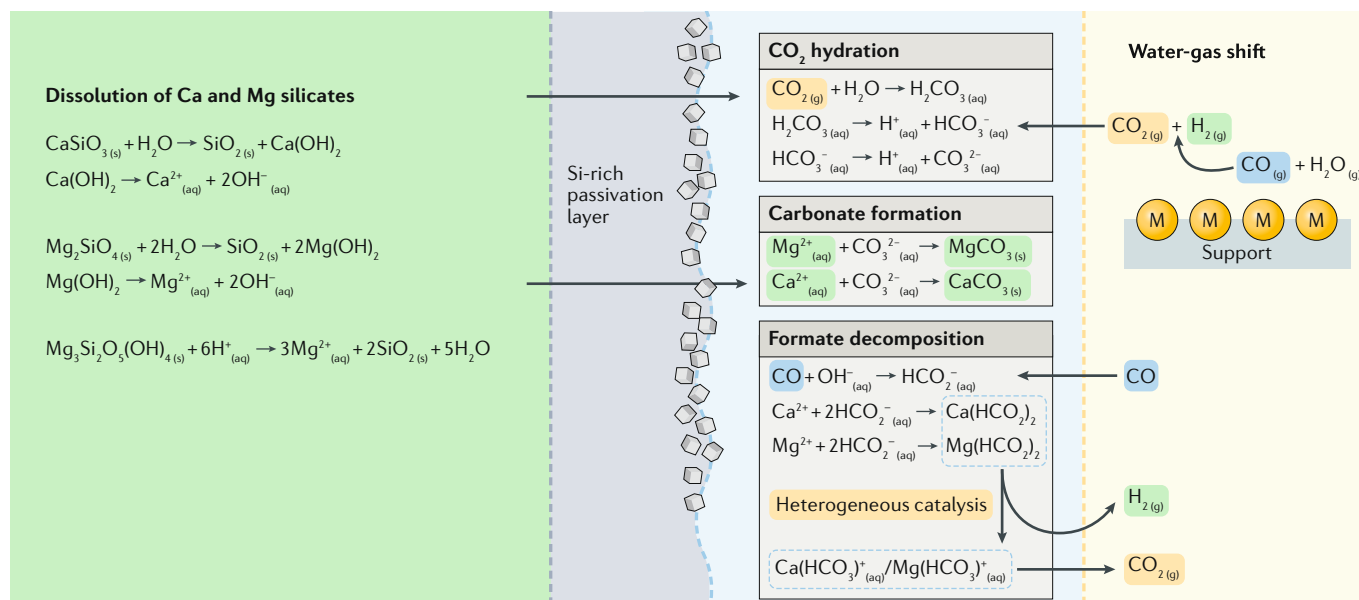


**Fig. 6 | Coupled reaction pathways in the conversion of silicates into carbonates and H<sub>2</sub>.** In principle, all reactions are reversible<sup>69</sup>. Reactions associated with the dissolution of silicates afford Ca<sup>2+</sup> and Mg<sup>2+</sup>, which combine with CO<sub>3</sub><sup>2-</sup> that, in turn, forms from CO<sub>2</sub>, a product of the water-gas shift reaction. Formates can also be produced and they undergo catalytic decomposition into bicarbonates and H<sub>2</sub>.

and calcite at these conditions is another consideration. Magnesite and calcite are generally thermally stable at temperatures up to 350 °C (REF.<sup>9</sup>) and 600 °C (REF.<sup>102</sup>) — well above the temperature range of 200–250 °C for the low-temperature WGSR.

A thermodynamics approach to evaluating a given set of reaction pathways involves summing the enthalpy changes of the coupled pathways as per Hess' law. Coupling the WGSR with the conversion of Mg<sub>2</sub>SiO<sub>4</sub> into MgCO<sub>3</sub> or CaSiO<sub>3</sub> into CaCO<sub>3</sub> yields an overall reaction that is exothermic ( $\Delta H < 0$ ; TABLE 1). The scheme of coupled reaction pathways that direct the synthesis of H<sub>2</sub> with inherent capture, conversion and storage of CO<sub>2</sub> as CaCO<sub>3</sub> and MgCO<sub>3</sub> is presented in FIG. 6. In addition to incorporating CO<sub>2</sub> hydration, mineral dissolution and the formation of calcium and magnesium carbonates, the scheme also features reactions associated with the decomposition of metal formate (for example, HCO<sub>2</sub>K) to H<sub>2</sub>. It was noted above that the decomposition is catalysed by 5–10% Pd on activated C, and it turns out that homogeneous catalysts such as metal carbonyls are also active<sup>103–106</sup>. As I have stressed so far, the primary advantage of reactive separation pathways is that CO<sub>2</sub> capture shifts the thermodynamic equilibrium to the products side, thereby enhancing H<sub>2</sub> production.

### Knowledge gaps

Achieving predictive control over coupled reaction pathways for integrated and low-temperature CO<sub>2</sub> capture, conversion and storage and the directed synthesis of H<sub>2</sub> by carbon mineralization will require greater understanding of multiphase and coupled reaction chemistry. Conventional approaches to elucidating kinetics of coupled reaction pathways often involve the iterative process of evaluating multiple process variables and quantifying bulk chemical compositions. These data are then used

to infer the underlying reaction mechanisms. Instead, transformative experimental methods are needed to directly probe the chemistry occurring due to fluid interactions with the alkaline solid interfaces. The key knowledge gaps and approaches to elucidate non-equilibrium and transient chemical events contributing to the changes in the bulk reaction kinetics are described in the following sections.

### Evolving chemistry at solid interfaces contributes to unexpected changes in extents of carbon mineralization.

Understanding and controlling the alkalinity changes in the solid and aqueous phases are often complicated because Ca<sup>2+</sup> and Mg<sup>2+</sup> dissolution from silicate surfaces is fast but is accompanied by slow mass-transfer-limited kinetics that occur over longer timescales. These different kinetic regimes have been characterized for the dissolution of (Mg,Fe)<sub>3</sub>Si<sub>2</sub>O<sub>5</sub>(OH)<sub>4</sub> (antigorite, a mineral from the serpentine family)<sup>100</sup>. In this model, labile Mg<sup>2+</sup> ions are rapidly released into the pore water of minerals (for example, Mg(OH)<sub>2</sub> (brucite) or Mg<sub>6</sub>Al<sub>2</sub>(CO<sub>3</sub>)<sub>2</sub>(OH)<sub>16</sub>·4H<sub>2</sub>O (hydrotalcites) and from the outer surfaces of serpentine), alkaline residues and tailings at atmospheric temperature and pressure<sup>107,108</sup>. Another challenge in developing predictive controls on the extraction of Ca<sup>2+</sup> and Mg<sup>2+</sup> into solution is the growth of mass transfer limiting passivation layers on the surfaces of the alkaline substrates. These passivation layers can include layers of carbonates or SiO<sub>2</sub> that are either less reactive or limit fluid access to the inner reacting surfaces<sup>21–23,109</sup>. There are uncertainties as to how passivating a surface affects carbon mineralization. For example, a stirred suspension of olivine ((Mg,Fe)<sub>2</sub>SiO<sub>4</sub>) in aqueous NaCl (1.0 M) and NaHCO<sub>3</sub> (0.64 M) at 185 °C under CO<sub>2</sub> (139 atm) exhibits 85% carbon mineralization after 3 h, suggesting that the SiO<sub>2</sub> by-product that precipitates does not

limit reactivity<sup>9</sup>. Contrarily, other studies have suggested that reactions performed with slow flow rates see the precipitation of secondary-reaction-limiting phases, such as  $\text{SiO}_2$ <sup>109</sup>.

Aside from the contrasting timescales of the processes involved in carbon mineralization, one must also consider competing precipitation reactions, particularly when multi-mineral alkaline resources such as industrial residues are used. When starting with Ca-bearing and Mg-bearing rocks such as anorthosite and basalt as the alkaline precursors<sup>101</sup>, carbon mineralization is hindered by the precipitation of Mg-bearing clays. For example,  $\text{Mg}^{2+}$  ions preferentially end up in Mg-bearing clays as opposed to the targeted magnesium carbonate phases, and the clay precipitates can contribute to mass-transfer-limiting passivation behaviour. We must also consider the amines used to capture and transfer  $\text{CO}_2$ , which can be degraded by impurities such as  $\text{SO}_x$  or  $\text{NO}_x$  and by thermal cycling at high temperatures. Despite the sensitivity of amines, the influence of impurities on the performance of amines in processing  $\text{CO}_2$  to give Ca-bearing and Mg-bearing carbonate precipitates is not well understood.

It is important to distinguish the formation of carbonate phases and secondary phases including  $\text{SiO}_2$ , a task that is, nowadays, often achieved using high-resolution scanning electron microscopy, transmission electron microscopy and atomic force microscopy. Likewise, to understand the growth of crystalline phases at solid interfaces, we turn to in operando grazing-incidence small-angle X-ray scattering (GI-SAXS)<sup>110,111</sup>. Lastly, to probe fluid-driven changes on solid interfaces, we can use in situ sum-frequency vibrational spectroscopy<sup>112</sup> and ambient-pressure X-ray photoelectron spectroscopy<sup>113</sup>, methods that have benefited from recent advancements. A more detailed description of analytical tools is given in a later section.

**Directing synthesis of  $\text{CaCO}_3$  and  $\text{MgCO}_3$  with structural and morphological specificity.** The complexity of multiphase reactions contributes to the challenge of producing  $\text{CaCO}_3$  and  $\text{MgCO}_3$  with structural and morphological specificity. Differences in fluid saturation and chemical composition, chemistry and morphology of the solid alkaline precursor, as well as temperature and flow conditions, influence the emergence of single or multiple crystalline phases. For example, carbon mineralization by looping with alkaline MEA solution converts CaO to calcite, vaterite and aragonite as the carbonate phases, while precursors such as  $\text{CaCl}_2$  yield calcite alone<sup>49</sup>. Under similar experimental conditions, starting with MgO results in metastable hydrated phases  $\text{MgCO}_3 \cdot x\text{H}_2\text{O}$ <sup>59</sup>. The higher likelihood of producing stable  $\text{CaCO}_3$  as opposed to  $\text{MgCO}_3$  is attributed to the lower charge density and less stable hydration spheres of  $\text{Ca}^{2+}$  ions compared with  $\text{Mg}^{2+}$  ions — the enhanced lability of  $\text{Ca}^{2+}$  helps the formation of the thermodynamic product (as noted above,  $\text{CaCO}_3$  precipitation rates are about six orders of magnitude greater than  $\text{MgCO}_3$ )<sup>53,114</sup>. One suggested approach to disrupting the stable hydration shell of  $\text{Mg}^{2+}$  ions is to direct the synthesis of  $\text{MgCO}_3$  at room temperature with polystyrene microspheres featuring carboxylate groups<sup>115</sup>.

These carboxylate groups disrupt the hydration shell and allow for the  $\text{Mg}^{2+}$  to bind to the carbonate species.

This approach lowers kinetic barriers for carbonate formation<sup>115</sup>. Such innovative approaches allow us to explore the feasibility of directing the synthesis of stable carbonate phases in ‘realistic’ multiphase environments comprising multiple ionic species.

Being Brønsted bases, it will not come as a surprise that the formation of solid carbonates is pH dependent. In the case of  $\text{Ca}^{2+}$ , when  $\text{pH} > 12$ , one observes the formation of stable calcite phases, with metastable aragonite and vaterite being favoured at  $\text{pH} \sim 11$  and  $\text{pH} < 10$ , respectively<sup>116,117</sup>. The phase obtained also depends on where it grows and, in amorphous cylindrical pores of track-etch membranes, one can observe amorphous  $\text{CaCO}_3$  converting into rod-shaped single calcite crystals<sup>118</sup>. In contrast, crosslinked gelatin films containing peptides such as poly(L-aspartate) and poly(L-glutamate) template the synthesis of metastable vaterite<sup>119</sup>, as does mixing  $\text{CaCl}_2$  and urea (a  $\text{CO}_3^{2-}$  source) in the presence of solvents such as ethylene glycol, 1,2-propanediol and glycerol at temperatures in the range 80–190 °C (REF.<sup>120</sup>). Instead, metastable aragonite can be synthesized by ultrasonication of  $\text{Ca}(\text{HCO}_3)_2$  (REF.<sup>121</sup>) using reverse surfactant microemulsions<sup>122</sup> or self-assembled monolayers as substrates<sup>123</sup> or by diffusion of  $\text{CO}_2$  into a solution of  $\text{CaCl}_2$  mixed with particles of a hydrophilic triblock copolymer. The latter process mimics biomineralization<sup>124</sup> of aragonite and, aside from using synthetic polymers, it is also possible to use biopolymers (proteins) to direct the formation of the metastable aragonite product<sup>125–128</sup>. Hydrophilic, aspartic-acid-rich macromolecules on the surfaces of shells have been known to influence the formation of aragonite<sup>125</sup>. Understanding these biomacromolecular influences on the directed synthesis of aragonite phases may allow us to develop advanced insights into the use of similar molecules for the reactive separation of  $\text{CO}_2$  via carbonate formation.

With respect to carbon mineralization using  $\text{Mg}^{2+}$ -containing materials, under ambient temperature and pressure, one obtains hydrated  $\text{MgCO}_3$  phases such as  $\text{MgCO}_3 \cdot 3\text{H}_2\text{O}$ <sup>129–133</sup>, and only subsequent heating affords anhydrous  $\text{MgCO}_3$  (magnesite) as the thermodynamic product<sup>134</sup>. Indeed, hydrothermal environments (high  $T$ ,  $p(\text{CO}_2)$  and salinity) accelerate the conversion of hydrated and metastable  $\text{MgCO}_3 \cdot x\text{H}_2\text{O}$  species into stable magnesite<sup>27,130,135,136</sup>. It is, thus, possible to selectively make a carbonate phase by starting with materials of known morphologies and fluid environments of known compositions. However, when carbon mineralization occurs in multiphase chemical environments, it becomes challenging to predict which carbonate phase will form. Thus, if we are to generate  $\text{H}_2$  from the WGS by the present carbon-mineralization method, we need a detailed understanding of how the multiple and different solid interfaces influence the growth of carbonate phases. For example, as mentioned above, carbonate growth on  $\text{MgCO}_3$  is favoured over  $\text{Mg}(\text{OH})_2$  due to higher self-adhesion and larger misfit between the two phases<sup>71</sup>. In systems starting with  $\text{Mg}_2\text{SiO}_4$  and/or  $\text{CaSiO}_3$ , we must consider how the  $\text{SiO}_2$ -bearing



co-product surfaces and their evolving porosity will affect the synthesis of carbonate phases. For example, experiments using nanoporous, amorphous  $\text{SiO}_2$  allow one to study how coating the pores with a self-assembled monolayer of organic groups with pendant anhydrides (which, like carboxylates, bind metal ions and accelerate mineralization) affects the pore sizes in which calcite chooses to crystallize<sup>137</sup>. Being now aware of the need to identify the evolving and transient nature of the solid interfaces and the fluidic environment, let us turn our attention to in operando characterization approaches.

**Characterizing chemo-morphological coupling in multiphase reaction environments.** Identifying and tuning the rate-limiting steps is essential for any chemical process and the same goes for designing multiphase chemical reaction pathways for reactive separation of  $\text{CO}_2$  and directed synthesis of clean energy carriers. The conventional approach of inferring underlying mechanisms from bulk kinetics measurements does not enable direct characterization of transient species and the transformations that give metastable or stable phases. I have, so far, discussed the chemistry at play but have not described many of the analytical tools required to arrive at these conclusions. It turns out that advancements in cross-scale synchrotron characterization techniques now allow us to probe the structural

and microstructural changes in materials from the sub-nanometre to the micrometre scales (FIG. 7). These X-ray techniques, in conjunction with neutron scattering and microscopy, afford us many capabilities. For example, recent advancements in ultrafast simultaneous characterization of structure and microstructure from the sub-nanometre to micrometre scales in less than 3 min using synchrotron ultra-small-angle, small-angle and wide-angle X-ray scattering (USAXS/SAXS/WAXS) measurements allow us to follow rapid kinetics over four orders of magnitude in space<sup>138–141</sup>. Local structural changes associated with  $\text{Ca}^{2+}$  and  $\text{Mg}^{2+}$  coordination in solid samples due to the presence of various aqueous solvents<sup>142–147</sup> are conveniently probed using X-ray absorption spectroscopy. The influence of surface chemistry and morphology on the nucleation and growth of carbonate phases under reaction conditions can be evaluated using GI-SAXS. Collectively, total scattering, X-ray absorption spectroscopy and GI-SAXS measurements can explain why hydrated phases  $\text{MgCO}_3 \cdot x\text{H}_2\text{O}$  are favoured at temperatures below 100 °C, while anhydrous  $\text{MgCO}_3$  is formed at higher temperatures. Atom-efficient utilization of silicate-bearing resources calls for exploring the chemical and morphological fate of  $\text{SiO}_2$  in relation to its influence in limiting or enhancing the reactivity of Ca-bearing or Mg-bearing minerals. These insights will be developed by probing reacted interfacial structures using in situ X-ray reflectivity, crystal truncation rod measurements and layer-by-layer evolution in the morphology and thickness of  $\text{SiO}_2$  layers as determined using atomic force microscopy and transmission electron microscopy. The evolution of the pore–solid networks and its dynamic influence on reactivity are best imaged using in operando microtomography and USAXS/SAXS. Lastly, to simultaneously evaluate changes in the solid-state chemistry, morphology and fluid composition, we need novel, multiphase reactors compatible with synchrotron measurements of the solid environment, as well as with online gas chromatography and mass spectrometry. In this way, advancing in operando characterization of multiphase chemical reactions may unlock the underlying mechanisms and provide a rational basis for tuning targeted chemical transformations.

Scalable and economical implementation of carbon-mineralization pathways for the reactive separation of  $\text{CO}_2$  is possible by addressing several fundamental research challenges associated with important knowledge gaps. Identifying rate-limiting steps and then rationally designing reaction pathways in a single reaction environment to overcome slow kinetic steps will be key to advancing present methods for reactive separation of  $\text{CO}_2$ . Further, multiphase chemical environments need to be designed to overcome challenges associated with the heterogeneous compositions of alkaline industrial residues and naturally-occurring minerals and rocks and heterogeneous compositions of acidic gas streams bearing not only  $\text{CO}_2$  but also  $\text{SO}_x$ ,  $\text{NO}_x$  and  $\text{H}_2\text{S}$ . Resolving these scientific challenges will bring us closer to commercially implementing low-cost, thermodynamically downhill and kinetically fast pathways for the sequestration of  $\text{CO}_2$  by carbon mineralization.

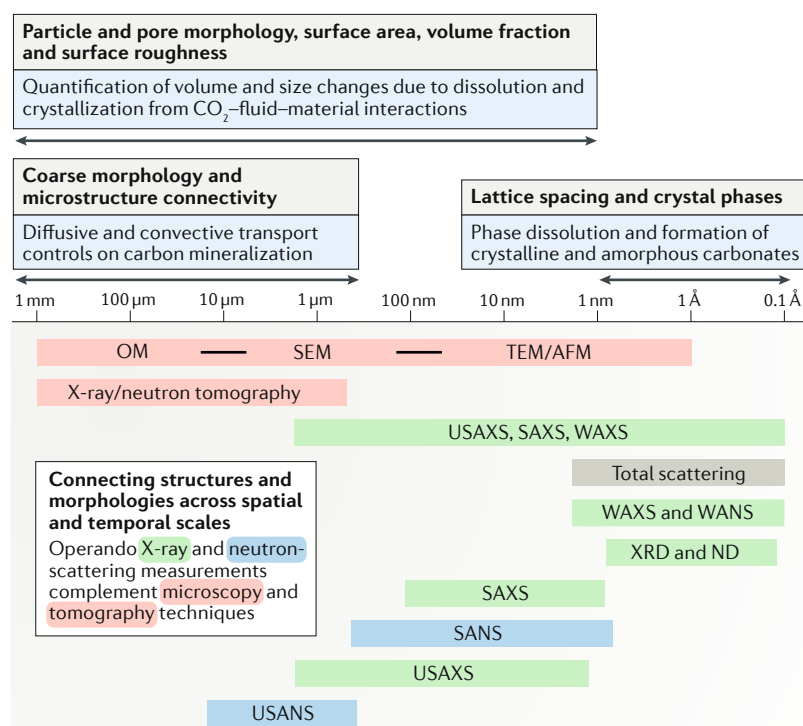


**Fig. 7 | Characterization over multiple length scales reveals reaction-induced chemo-morphological coupling.** X-ray and neutron-scattering methods, complemented by microscopy and tomography, enable us to probe features on the sub-nanometre to millimetre scales<sup>140</sup>. AFM, atomic force microscopy; ND, neutron diffraction; OM, optical microscopy; SANS, small-angle neutron scattering; SAXS, small-angle X-ray scattering; SEM, scanning electron microscopy; TEM, transmission electron microscopy; USANS, ultra-small-angle neutron scattering; USAXS, ultra-small-angle X-ray scattering; WANS, wide-angle neutron scattering; WAXS, wide-angle X-ray scattering; XRD, X-ray diffraction.

# Conclusions

In this Review, I have explored carbon mineralization as a pathway for the reactive separation of CO<sub>2</sub> from point-source emissions and the directed synthesis of clean energy carriers, such as H<sub>2</sub>. Integrated single-step pathways of CO<sub>2</sub> capture and conversion pathways have conventionally been explored for the synthesis of organic chemicals<sup>142,143</sup>. In this Review, we discuss cohesive and rational approaches to design reaction pathways for the capture and conversion of CO<sub>2</sub> into inorganic calcium and magnesium carbonates, and the directed synthesis of H<sub>2</sub>. The thermodynamically downhill nature of carbon mineralization can only be exploited with kinetically accessible reaction pathways. In one approach, the use of nucleophiles such as amines or amino-acid salts allows us to overcome challenges associated with the low solubility of CO<sub>2</sub> in the aqueous phase. High concentrations of dissolved carbonate aid the precipitation of calcium and magnesium carbonates at temperatures below 50 °C. The regeneration of the amine or amino-acid nucleophile accompanies carbonate precipitation and allows reuse of the aqueous medium. In another distinct approach, the feasibility of achieving high

conversions of CaSiO<sub>3</sub> and Mg<sub>2</sub>SiO<sub>4</sub> into calcium and magnesium carbonates under conditions that favour the WGSR allows us to couple these reactions to the directed synthesis of H<sub>2</sub> with the capture of CO<sub>2</sub>. Older studies explored the use of oxides and hydroxides of Ca and Mg as alkaline sources to trap CO<sub>2</sub> and accompany H<sub>2</sub> synthesis. More recent work exploits the high reactivity of CaSiO<sub>3</sub> and Mg<sub>2</sub>SiO<sub>4</sub> under relevant experimental conditions to demonstrate the promising potential for using these earth-abundant minerals. To broaden the scope of these reaction pathways to incorporate a wide range of alkaline feedstocks with varying chemistries, we require improvements of present in operando spectroscopy and scattering characterization methods to develop the interfacial chemical basis for the observed structures and morphologies of carbonates. This will allow us to unravel the mechanisms operative in multiphase reaction pathways and, in the present case, enable atom-efficient and energy-efficient capture, conversion and storage of CO<sub>2</sub> and the directed synthesis of H<sub>2</sub>, along with the formation of CaCO<sub>3</sub> or MgCO<sub>3</sub>.

Published online: 14 January 2020

- Kelemen, P. B. et al. Rates and mechanisms of mineral carbonation in peridotite: natural processes and recipes for enhanced, in situ CO<sub>2</sub> capture and storage. *Annu. Rev. Earth Planet. Sci.* **39**, 545–576 (2011).
- Kelemen, P. B. & Matter, J. In situ carbonation of peridotite for CO<sub>2</sub> storage. *Proc. Natl Acad. Sci. USA* **105**, 17295–17300 (2008).
- Matter, J. M. & Kelemen, P. B. Permanent storage of carbon dioxide in geological reservoirs by mineral carbonation. *Nat. Geosci.* **2**, 837–841 (2009).
- Harrison, A. L., Power, I. M. & Dipple, G. M. Accelerated carbonation of brucite in mine tailings for carbon sequestration. *Environ. Sci. Technol.* **47**, 126–134 (2013).
- Matter, J. M. et al. Rapid carbon mineralization for permanent disposal of anthropogenic carbon dioxide emissions. *Science* **352**, 1312–1314 (2016).
- Schaefer, H. T., McGrail, B. P. & Owen, A. T. Basalt-CO<sub>2</sub>-H<sub>2</sub>O interactions and variability in carbonate mineralization rates. *Energy Procedia* **1**, 4899–4906 (2009).
- Schaefer, H. T., McGrail, B. P., Owen, A. T. & Arey, B. W. Mineralization of basalts in the CO<sub>2</sub>-H<sub>2</sub>O-H<sub>2</sub>S system. *Int. J. Greenh. Gas Control* **16**, 187–196 (2013).
- Gerdemann, S. J., O'Connor, W. K., Dahlin, D. C., Penner, L. R. & Rush, H. Ex situ aqueous mineral carbonation. *Environ. Sci. Technol.* **41**, 2587–2593 (2007).
- Gadikota, G., Matter, J., Kelemen, P. & Park, A.-H. A. Chemical and morphological changes during olivine carbonation for CO<sub>2</sub> storage in the presence of NaCl and NaHCO<sub>3</sub>. *Phys. Chem. Chem. Phys.* **16**, 4679–4693 (2014).
- Eikeland, E., Blichfeld, A. B., Tyrsted, C., Jensen, A. & Iversen, B. B. Optimized carbonation of magnesium silicate mineral for CO<sub>2</sub> storage. *ACS Appl. Mater. Interfaces* **7**, 5258–5264 (2015).
- Miller, Q. R. et al. Quantitative review of olivine carbonation kinetics: reactivity trends, mechanistic insights, and research frontiers. *Environ. Sci. Technol. Lett.* **6**, 431–442 (2019).
- Wang, F., Dreisinger, D., Jarvis, M., Hitchins, T. & Dyson, D. Quantifying kinetics of mineralization of carbon dioxide by olivine under moderate conditions. *Chem. Eng. J.* **360**, 452–463 (2019).
- National Academies of Sciences, Engineering, and Medicine. Negative Emissions Technologies and Reliable Sequestration: A Research Agenda. *The National Academies Press* <https://www.nap.edu/catalog/25259/negative-emissions-technologies-and-reliable-sequestration-a-research-agenda> (2019).
- Palandri, J. L. & Kharaka, Y. K. A compilation of rate parameters of water-mineral interaction kinetics for application to geochemical modeling. *U.S. Geological Survey Open File Report 2004-1068* <https://pubs.usgs.gov/of/2004/1068/> (2004).
- Bénézet, P., Saldi, G. D., Dandurand, J.-L. & Schott, J. Experimental determination of the solubility product of magnesite at 50 to 200 °C. *Chem. Geol.* **286**, 21–31 (2011).
- Weyl, P. The change in solubility of calcium carbonate with temperature and carbon dioxide content. *Geochim. Cosmochim. Acta* **17**, 214–225 (1959).
- Rhodes, C., Hutchings, G. J. & Ward, A. M. Water-gas shift reaction: finding the mechanistic boundary. *Catal. Today* **23**, 43–58 (1995).
- Mirjafari, P., Asghari, K. & Mahinpey, N. Investigating the application of enzyme carbonic anhydrase for CO<sub>2</sub> sequestration purposes. *Ind. Eng. Chem. Res.* **46**, 921–926 (2007).
- Patel, T. N., Park, A.-H. A. & Banta, S. Periplasmic expression of carbonic anhydrase in *Escherichia coli*: a new biocatalyst for CO<sub>2</sub> hydration. *Biotechnol. Bioeng.* **110**, 1865–1873 (2013).
- Zhao, H., Park, Y., Lee, D. H. & Park, A.-H. A. Tuning the dissolution kinetics of wollastonite via chelating agents for CO<sub>2</sub> sequestration with integrated synthesis of precipitated calcium carbonates. *Phys. Chem. Chem. Phys.* **15**, 15185–15192 (2013).
- Béarat, H. et al. Carbon sequestration via aqueous olivine mineral carbonation: role of passivating layer formation. *Environ. Sci. Technol.* **40**, 4802–4808 (2006).
- Daval, D. et al. Influence of amorphous silica layer formation on the dissolution rate of olivine at 90 °C and elevated pCO<sub>2</sub>. *Chem. Geol.* **284**, 193–209 (2011).
- Daval, D. et al. in *Proc. 13th Int. Conf. Water Rock Interaction WRI-13* (eds Birkle, P. & Torres-Alvarado, I. S.) 713–716 (Taylor & Francis, 2010).
- Park, A.-H. A. et al. Methods and systems for capturing and storing carbon dioxide. US Patent 14/237,690 (2015).
- Di Lorenzo, F. et al. The carbonation of wollastonite: a model reaction to test natural and biomimetic catalysts for enhanced CO<sub>2</sub> sequestration. *Minerals* **8**, 209 (2018).
- Giammar, D. E., Bruant Jr, R. G. & Peters, C. A. Forsterite dissolution and magnesite precipitation at conditions relevant for deep saline aquifer storage and sequestration of carbon dioxide. *Chem. Geol.* **217**, 257–276 (2005).
- Swanson, E. J., Fricker, K. J., Sun, M. & Park, A.-H. A. Directed precipitation of hydrated and anhydrous magnesium carbonates for carbon storage. *Phys. Chem. Chem. Phys.* **16**, 23440–23450 (2014).
- Yu, C.-H., Huang, C.-H. & Tan, C.-S. A review of CO<sub>2</sub> capture by absorption and adsorption. *Aerosol Air Qual. Res.* **12**, 745–769 (2012).
- Rochelle, G. T. Amine scrubbing for CO<sub>2</sub> capture. *Science* **325**, 1652–1654 (2009).
- Bottoms, R. R. Process for separating acidic gases. US Patent 1,834,016 (1930).
- Lepaumier, H., Picq, D. & Carrette, P.-L. New amines for CO<sub>2</sub> capture. I. mechanisms of amine degradation in the presence of CO<sub>2</sub>. *Ind. Eng. Chem. Res.* **48**, 9061–9067 (2009).
- Sayari, A., Heydari-Gorji, A. & Yang, Y. CO<sub>2</sub>-induced degradation of amine-containing adsorbents: reaction products and pathways. *J. Am. Chem. Soc.* **134**, 13834–13842 (2012).
- Gouedard, C., Picq, D., Launay, F. & Carrette, P.-L. Amine degradation in CO<sub>2</sub> capture. I. A review. *Int. J. Greenh. Gas Control* **10**, 244–270 (2012).
- Martin, S. et al. New amines for CO<sub>2</sub> capture. IV. Degradation, corrosion, and quantitative structure property relationship model. *Ind. Eng. Chem. Res.* **51**, 6283–6289 (2012).
- Dai, N. et al. Measurement of nitrosamine and nitramine formation from NO<sub>x</sub> reactions with amines during amine-based carbon dioxide capture for postcombustion carbon sequestration. *Environ. Sci. Technol.* **46**, 9793–9801 (2012).
- Dai, N. & Mitch, W. A. Controlling nitrosamines, nitramines, and amines in amine-based CO<sub>2</sub> capture systems with continuous ultraviolet and ozone treatment of wastewater. *Environ. Sci. Technol.* **49**, 8878–8886 (2015).
- Wang, Z. & Mitch, W. A. Influence of dissolved metals on N-nitrosamine formation under amine-based CO<sub>2</sub> capture conditions. *Environ. Sci. Technol.* **49**, 11974–11981 (2015).
- Rochelle, G. T. Thermal degradation of amines for CO<sub>2</sub> capture. *Curr. Opin. Chem. Eng.* **1**, 183–190 (2012).
- Soosaiprakasham, I. R. & Veawab, A. Corrosion and polarization behavior of carbon steel in MEA-based CO<sub>2</sub> capture process. *Int. J. Greenh. Gas Control* **2**, 553–562 (2008).
- Xiang, Y., Choi, Y. S., Yang, Y. & Nešić, S. Corrosion of carbon steel in MDEA-based CO<sub>2</sub> capture plants under regenerator conditions: Effects of O<sub>2</sub> and heat-stable salts. *Corrosion* **71**, 30–37 (2014).
- Wattanaphan, P., Sema, T., Idem, R., Liang, Z. & Tontiwachwuthikul, P. Effects of flue gas composition on carbon steel (1020) corrosion in MEA-based CO<sub>2</sub> capture process. *Int. J. Greenh. Gas Control* **19**, 340–349 (2013).
- Veawab, A., Tontiwachwuthikul, P. & Chakma, A. Corrosion behavior of carbon steel in the CO<sub>2</sub> absorption process using aqueous amine solutions. *Ind. Eng. Chem. Res.* **38**, 3917–3924 (2002).
- Kittel, J. et al. Corrosion in MEA units for CO<sub>2</sub> capture: pilot plant studies. *Energy Procedia* **1**, 791–797 (2009).
- Mandal, B. P., Guha, M., Biswas, A. K. & Bandyopadhyay, S. S. Removal of carbon dioxide

- by absorption in mixed amines: modelling of absorption in aqueous MDEA/MEA and AMP/MEA solutions. *Chem. Eng. Sci.* **56**, 6217–6224 (2001).
45. Idem, R. et al. Pilot plant studies of the CO<sub>2</sub> capture performance of aqueous MEA and mixed MEA/MDEA solvents at the University of Regina CO<sub>2</sub> capture technology development plant and the boundary dam CO<sub>2</sub> capture demonstration plant. *Ind. Eng. Chem. Res.* **45**, 2414–2420 (2006).
  46. Li, Q. et al. A novel strategy for carbon capture and sequestration by rHLPD processing. *Front. Energy Res.* **3**, 53 (2016).
  47. Ji, L. et al. Integrated absorption-mineralisation for low-energy CO<sub>2</sub> capture and sequestration. *Appl. Energy* **225**, 356–366 (2018).
  48. Kang, J. M. et al. Energy-efficient chemical regeneration of AMP using calcium hydroxide for operating carbon dioxide capture process. *Chem. Eng. J.* **335**, 338–344 (2018).
  49. Arti, M. et al. Single process for CO<sub>2</sub> capture and mineralization in various alkanolamines using calcium chloride. *Energy Fuels* **31**, 763–769 (2017).
  50. Yu, B. et al. Coupling a sterically hindered amine-based absorption and coal fly ash triggered amine regeneration: a high energy-saving process for CO<sub>2</sub> absorption and sequestration. *Int. J. Greenh. Gas Control* **87**, 58–65 (2019).
  51. Vaidya, P. D., Konduru, P., Vaidyanathan, M. & Kenig, E. Y. Kinetics of carbon dioxide removal by aqueous alkaline amino acid salts. *Ind. Eng. Chem. Res.* **49**, 11067–11072 (2010).
  52. Kumar, P. S., Hogendoorn, J. A., Versteeg, G. F. & Feron, P. H. M. Kinetics of the reaction of CO<sub>2</sub> with aqueous potassium salt of taurine and glycine. *AIChE J.* **49**, 203–213 (2003).
  53. Portugal, A. F., Sousa, J. M., Magalhães, F. D. & Mendes, A. Solubility of carbon dioxide in aqueous solutions of amino acid salts. *Chem. Eng. Sci.* **64**, 1993–2002 (2009).
  54. Portugal, A. F., Derks, P. W. J., Versteeg, G. F., Magalhães, F. D. & Mendes, A. Characterization of potassium glycinate for carbon dioxide absorption purposes. *Chem. Eng. Sci.* **62**, 6534–6547 (2007).
  55. Guo, D. et al. Amino acids as carbon capture solvents: chemical kinetics and mechanism of the glycine+CO<sub>2</sub> reaction. *Energy Fuels* **27**, 3898–3904 (2013).
  56. Thee, H. et al. A kinetic study of CO<sub>2</sub> capture with potassium carbonate solutions promoted with various amino acids: glycine, sarcosine and proline. *Int. J. Greenh. Gas Control* **20**, 212–222 (2014).
  57. Sanchez Fernandez, E. et al. Conceptual design of a novel CO<sub>2</sub> capture process based on precipitating amino acid solvents. *Ind. Eng. Chem. Res.* **52**, 12223–12235 (2013).
  58. Sanchez-Fernandez, E. et al. New process concepts for CO<sub>2</sub> capture based on precipitating amino acids. *Energy Procedia* **37**, 1160–1171 (2013).
  59. Majchrowicz, M. E., Brilman, D. W. F. (Wim) & Groeneweld, M. J. Precipitation regime for selected amino acid salts for CO<sub>2</sub> capture from flue gases. *Energy Procedia* **1**, 979–984 (2009).
  60. Sanchez-Fernandez, E. et al. Analysis of process configurations for CO<sub>2</sub> capture by precipitating amino acid solvents. *Ind. Eng. Chem. Res.* **53**, 2348–2361 (2014).
  61. Hänchen, M., Prigiobbe, V., Storti, G., Seward, T. M. & Mazzotti, M. Dissolution kinetics of forsterite olivine at 90–150 °C including effects of the presence of CO<sub>2</sub>. *Geochim. Cosmochim. Acta* **70**, 4403–4416 (2006).
  62. Oelkers, E. H., Declercq, J., Saldi, G. D., Gislason, S. R. & Schott, J. Olivine dissolution rates: a critical review. *Chem. Geol.* **500**, 1–19 (2018).
  63. Kirchofer, A., Brandt, A., Krevor, S., Prigiobbe, V. & Wilcox, J. Impact of alkalinity sources on the life-cycle energy efficiency of mineral carbonation technologies. *Energy Environ. Sci.* **5**, 8631–8641 (2012).
  64. Park, A.-H. A. & Fan, L.-S. CO<sub>2</sub> mineral sequestration: physically activated dissolution of serpentine and pH swing process. *Chem. Eng. Sci.* **59**, 5241–5247 (2004).
  65. Sanna, A., Hall, M. R. & Maroto-Valer, M. Post-processing pathways in carbon capture and storage by mineral carbonation (CCSM) towards the introduction of carbon neutral materials. *Energy Environ. Sci.* **5**, 7781–7796 (2012).
  66. Gadikota, G. & Park, A.-H. A. in *Carbon Dioxide Utilisation: Closing the Carbon Cycle* (eds Styring, P., Quadrelli, E. A. & Armstrong, K.) 115–137 (Elsevier, 2015).
  67. Murnandari, A. et al. Effect of process parameters on the CaCO<sub>3</sub> production in the single process for carbon capture and mineralization. *Korean J. Chem. Eng.* **34**, 935–941 (2017).
  68. Han, C. & Harrison, D. P. Simultaneous shift reaction and carbon dioxide separation for the direct production of hydrogen. *Chem. Eng. Sci.* **49**, 5875–5883 (1994).
  69. Liu, M. & Gadikota, G. Integrated CO<sub>2</sub> capture, conversion, and storage to produce calcium carbonate using an amine looping strategy. *Energy Fuels* **33**, 1722–1733 (2019).
  70. Liu, M., Asgar, H., Seifert, S. & Gadikota, G. Novel aqueous amine looping approach for the direct capture, conversion and storage of CO<sub>2</sub> to produce magnesium carbonate. *Sustain. Energy Fuels*. <https://doi.org/10.1039/C9SE00316A> (2019).
  71. Hövelmann, J., Putnis, C. V., Ruiz-Agudo, E. & Austrheim, H. Direct nanoscale observations of CO<sub>2</sub> sequestration during brucite [Mg(OH)<sub>2</sub>] dissolution. *Environ. Sci. Technol.* **46**, 5253–5260 (2012).
  72. Saldi, G. D., Jordan, G., Schott, J. & Oelkers, E. H. Magnesite growth rates as a function of temperature and saturation state. *Geochim. Cosmochim. Acta* **73**, 5646–5657 (2009).
  73. Schott, J., Pokrovsky, O. S. & Oelkers, E. H. The link between mineral dissolution/precipitation kinetics and solution chemistry. *Rev. Mineral Geochem.* **70**, 207–258 (2009).
  74. Dresselhaus, M. *Basic Research Needs for the Hydrogen Economy*. US Department of Energy (2003).
  75. Turner, J. A. Sustainable hydrogen production. *Science* **305**, 972–975 (2004).
  76. Pereira, E. G., da Silva, J. N., de Oliveira, J. L. & Machado, C. S. Sustainable energy: a review of gasification technologies. *Renew. Sustain. Energy Rev.* **16**, 4753–4762 (2012).
  77. Levalley, T. L., Richard, A. R. & Fan, M. The progress in water gas shift and steam reforming hydrogen production technologies — a review. *Int. J. Hydrog. Energy* **39**, 16983–17000 (2014).
  78. Bukur, D. B., Todici, B. & Elbashir, N. Role of water-gas-shift reaction in Fischer–Tropsch synthesis on iron catalysts: a review. *Catal. Today* **275**, 66–75 (2016).
  79. Fricker, K. J. *Magnesium Hydroxide Sorbents for Combined Carbon Dioxide Capture and Storage in Energy Conversion Systems*. PhD Thesis, Columbia Univ. (2014).
  80. Byron Smith, R. J., Loganathan, M. & Shantha, M. S. A review of the water gas shift reaction kinetics. *Int. J. Chem. React. Eng.* **8**, R4 (2010).
  81. Pal, D. B., Chand, R., Upadhyay, S. N. & Mishra, P. K. Performance of water gas shift reaction catalysts: a review. *Renew. Sustain. Energy Rev.* **93**, 549–565 (2018).
  82. Elliott, D. C. & Sealock Jr, L. J. Aqueous catalyst systems for the water-gas shift reaction. 1. Comparative catalyst studies. *Ind. Eng. Chem. Prod. Res. Dev.* **22**, 426–431 (1983).
  83. Elliott, D. C., Hallen, R. T. & Sealock Jr, L. J. Aqueous catalyst systems for the water-gas shift reaction. 2. Mechanism of basic catalysis. *Ind. Eng. Chem. Prod. Res. Dev.* **22**, 431–435 (1983).
  84. Onsager, O.-T., Brownrigg, M. S. A. & Lodeng, R. Hydrogen production from water and CO via alkali metal formate salts. *Int. J. Hydrog. Energy* **21**, 883–885 (1996).
  85. Stevens, R. W. Jr, Shamsi, A., Carpenter, S. & Siriwardane, R. Sorption-enhanced water gas shift reaction by sodium-promoted calcium oxides. *Fuel* **89**, 1280–1286 (2010).
  86. Beaver, M. G., Caram, H. S. & Sircar, S. Selection of CO<sub>2</sub> chemisorbent for fuel-cell grade H<sub>2</sub> production by sorption-enhanced water gas shift reaction. *Int. J. Hydrog. Energy* **34**, 2972–2978 (2009).
  87. Dasgupta, D., Mondal, K. & Wiltowski, T. Robust, high reactivity and enhanced capacity carbon dioxide removal agents for hydrogen production applications. *Int. J. Hydrog. Energy* **33**, 303–311 (2008).
  88. Ding, Y. & Alpay, E. Adsorption-enhanced steam–methane reforming. *Chem. Eng. Sci.* **55**, 3929–3940 (2000).
  89. Guoxin, H. & Hao, H. Hydrogen rich fuel gas production by gasification of wet biomass using a CO<sub>2</sub> sorbent. *Biomass Bioenergy* **33**, 899–906 (2009).
  90. Harrison, D. P. Sorption-enhanced hydrogen production: a review. *Ind. Eng. Chem. Res.* **47**, 6486–6501 (2008).
  91. Lee, K. B., Beaver, M. G., Caram, H. S. & Sircar, S. Reversible chemisorbents for carbon dioxide and their potential applications. *Ind. Eng. Chem. Res.* **47**, 8048–8062 (2008).
  92. Lopez Ortiz, A. & Harrison, D. P. Hydrogen production using sorption-enhanced reaction. *Ind. Eng. Chem. Res.* **40**, 5102–5109 (2002).
  93. Van Selow, E. R., Cobden, P. D., Verbraeken, P. A., Hufton, J. R. & van den Brink, R. W. Carbon capture by sorption-enhanced water–gas shift reaction process using hydrotalcite-based material. *Ind. Eng. Chem. Res.* **48**, 4184–4193 (2009).
  94. Xiu, G.-h., Li, P. & Rodrigues, A. E. Sorption-enhanced reaction process with reactive regeneration. *Chem. Eng. Sci.* **57**, 3893–3908 (2002).
  95. Wei, L., Xu, S., Liu, J., Liu, C. & Liu, S. Hydrogen production in steam gasification of biomass with CaO as a CO<sub>2</sub> absorbent. *Energy Fuels* **22**, 1997–2004 (2008).
  96. Fricker, K. J. & Park, A.-H. A. Effect of H<sub>2</sub>O on Mg(OH)<sub>2</sub> carbonation pathways for combined CO<sub>2</sub> capture and storage. *Chem. Eng. Sci.* **100**, 332–341 (2013).
  97. Fricker, K. J. & Park, A.-H. A. in *Proc. 12th Int. Conf. Gas-Liquid and Gas-Liquid-Solid Reactor Engineering (GLS 12)* (2015).
  98. O'Connor, W. K. et al. Carbon dioxide sequestration by direct mineral carbonation: results from recent studies and current status. *US Department of Energy DOE/ARC-2001-029* (2001).
  99. O'Connor, W. K., Dahlin, D. C., Rush, G. E., Gerdemann, S. J. & Nilsen, D. N. Final report: aqueous mineral carbonation. *US Department of Energy DOE/ARC-TR-04-002* (2004).
  100. Gadikota, G., Swanson, E. J., Zhao, H. & Park, A.-H. A. Experimental design and data analysis for accurate estimation of reaction kinetics and conversion for carbon mineralization. *Ind. Eng. Chem. Res.* **53**, 6664–6676 (2014).
  101. Gadikota, G. *Geo-chemo-physical Studies of Carbon Mineralization for Natural and Engineered Carbon Storage*. PhD Thesis, Columbia Univ. (2014).
  102. Rodriguez-Navarro, C., Ruiz-Agudo, E., Luque, A., Rodriguez-Navarro, A. B. & Ortega-Huertas, M. Thermal decomposition of calcite: mechanisms of formation and textural evolution of CaO nanocrystals. *Am. Mineral.* **94**, 578–593 (2009).
  103. Ungermann, C. et al. Homogeneous catalysis of the water gas shift reaction by ruthenium and other metal carbonyls. studies in alkaline solutions. *J. Am. Chem. Soc.* **101**, 5922–5929 (1979).
  104. King Jr, A. D., King, R. B. & Yang, D. B. Homogeneous catalysis of the water gas shift reaction using iron pentacarbonyl. *J. Am. Chem. Soc.* **102**, 1028–1032 (1980).
  105. Ishida, H., Tanaka, K., Morimoto, M. & Tanaka, T. Isolation of intermediates in the water gas shift reactions catalyzed by [Ru(bpy)<sub>3</sub>](CO)Cl<sup>+</sup> and [Ru(bpy)<sub>3</sub>](CO)<sub>2</sub><sup>2+</sup>. *Organometallics* **5**, 724–730 (1986).
  106. Laine, R. M. & Crawford, E. J. Homogeneous catalysis of the water-gas shift reaction. *J. Mol. Catal.* **44**, 357–387 (1988).
  107. Thom, J. G. M., Dipple, G. M., Power, I. M. & Harrison, A. L. Chrysotile dissolution rates: implications for carbon sequestration. *Appl. Geochem.* **35**, 244–254 (2013).
  108. Vanderzee, S. S., Dipple, G. M. & Bradshaw, P. M. D. Targeting highly reactive labile magnesium in ultramafic tailings for greenhouse-gas offsets and potential tailings stabilization at the Baptiste deposit, central British Columbia (NTS 093K/13, 14). *Geoscience BC* [http://cdn.geosciencebc.com/pdf/SummaryofActivities2018/MM/Schol\\_SoA2018\\_MM\\_Vanderzee.pdf](http://cdn.geosciencebc.com/pdf/SummaryofActivities2018/MM/Schol_SoA2018_MM_Vanderzee.pdf) (2019).
  109. King, H. E., Plümper, O. & Putnis, A. Effect of secondary phase formation on the carbonation of olivine. *Environ. Sci. Technol.* **44**, 6503–6509 (2010).
  110. Waychunas, G. A. Grazing-incidence X-ray absorption and emission spectroscopy. *Rev. Mineral. Geochem.* **49**, 267–315 (2002).
  111. Fernandez-Martinez, A., Hu, Y., Lee, B., Jun, Y.-S. & Waychunas, G. A. In situ determination of interfacial energies between heterogeneously nucleated CaCO<sub>3</sub> and quartz substrates: thermodynamics of CO<sub>2</sub> mineral trapping. *Environ. Sci. Technol.* **47**, 102–109 (2013).
  112. Jubb, A. M., Hua, W. & Allen, H. C. Environmental chemistry at vapor/water interfaces: insights from vibrational sum frequency generation spectroscopy. *Annu. Rev. Phys. Chem.* **63**, 107–130 (2012).
  113. Axnanda, S. et al. Using “tender” X-ray ambient pressure X-ray photoelectron spectroscopy as a direct probe of solid–liquid interface. *Sci. Rep.* **5**, 9788 (2015).
  114. Jiao, D., King, C., Grossfield, A., Darden, T. A. & Ren, P. Simulation of Ca<sup>2+</sup> and Mg<sup>2+</sup> solvation using polarizable atomic multipole potential. *J. Phys. Chem. B* **110**, 18553–18559 (2006).
  115. Power, I. M., Kenward, P. A., Dipple, G. M. & Raudsepp, M. Room temperature magnesite

- precipitation. *Cryst. Growth Des.* **17**, 5652–5659 (2017).
116. Tai, C. Y. & Chen, F.-B. Polymorphism of  $\text{CaCO}_3$ , precipitated in a constant-composition environment. *AIChE J.* **44**, 1790–1798 (1998).
117. Nebel, H. & Eppler, M. Continuous preparation of calcite, aragonite and vaterite, and of magnesium-substituted amorphous calcium carbonate (Mg-ACC). *Z. Anorg. Allg. Chem.* **634**, 1439–1443 (2008).
118. Loste, E., Park, R. J., Warren, J. & Meldrum, F. C. Precipitation of calcium carbonate in confinement. *Adv. Funct. Mater.* **14**, 1211–1220 (2004).
119. Falini, G., Fermani, S., Gazzano, M. & Ripamonti, A. Oriented crystallization of vaterite in collagenous matrices. *Chem. Eur. J.* **4**, 1048–1052 (1998).
120. Li, Q., Ding, Y., Li, F., Xie, B. & Qian, Y. Solvothermal growth of vaterite in the presence of ethylene glycol, 1, 2-propanediol and glycerol. *J. Cryst. Growth* **236**, 357–362 (2002).
121. Zhou, G.-T., Yu, J. C., Wang, X.-C. & Zhang, L.-Z. Sonochemical synthesis of aragonite-type calcium carbonate with different morphologies. *N. J. Chem.* **28**, 1027–1031 (2004).
122. Li, M., Lebeau, B. & Mann, S. Synthesis of aragonite nanofilament networks by mesoscale self-assembly and transformation in reverse microemulsions. *Adv. Mater.* **15**, 2032–2035 (2003).
123. Küther, J. et al. Templated crystallisation of calcium and strontium carbonates on centred rectangular self-assembled monolayer substrates. *Chem. Eur. J.* **4**, 1834–1842 (1998).
124. Nassif, N. et al. Synthesis of stable aragonite superstructures by a biomimetic crystallization pathway. *Angew. Chem. Int. Ed.* **44**, 6004–6009 (2005).
125. Belcher, A. M. et al. Control of crystal phase switching and orientation by soluble mollusc-shell proteins. *Nature* **381**, 56–58 (1996).
126. Falini, G., Albeck, S., Weiner, S. & Addadi, L. Control of aragonite or calcite polymorphism by mollusk shell macromolecules. *Science* **271**, 67–69 (1996).
127. Heywood, B. R. & Mann, S. Molecular construction of oriented inorganic materials: controlled nucleation of calcite and aragonite under compressed Langmuir monolayers. *Chem. Mater.* **6**, 311–318 (1994).
128. Litvin, A. L., Valiyaveetil, S., Kaplan, D. L. & Mann, S. Template-directed synthesis of aragonite under supramolecular hydrogen-bonded langmuir monolayers. *Adv. Mater.* **9**, 124–127 (1997).
129. Davies, P. J. & Bubela, B. The transformation of nesquehonite into hydromagnesite. *Chem. Geol.* **12**, 289–300 (1973).
130. Hänchen, M., Prigobbe, V., Baciocchi, R. & Mazzotti, M. Precipitation in the Mg-carbonate system—effects of temperature and  $\text{CO}_2$  pressure. *Chem. Eng. Sci.* **63**, 1012–1028 (2008).
131. Langmuir, D. Stability of carbonates in the system  $\text{MgO}-\text{CO}_2-\text{H}_2\text{O}$ . *J. Geol.* **73**, 730–754 (1965).
132. Zhang, Z. et al. Temperature- and pH-dependent morphology and FT-IR analysis of magnesium carbonate hydrates. *J. Phys. Chem. B* **110**, 12969–12973 (2006).
133. Zhao, L., Sang, L., Chen, J., Ji, J. & Teng, H. H. Aqueous carbonation of natural brucite: relevance to  $\text{CO}_2$  sequestration. *Environ. Sci. Technol.* **44**, 406–411 (2010).
134. Lanas, J. & Alvarez, J. I. Dolomitic lime: thermal decomposition of nesquehonite. *Thermochim. Acta* **421**, 123–132 (2004).
135. Sayles, F. L. & Fyfe, W. S. The crystallization of magnesite from aqueous solution. *Geochim. Cosmochim. Acta* **37**, 87–99 (1973).
136. Fricker, K. J. & Park, A.-H. A. Investigation of the different carbonate phases and their formation kinetics during  $\text{Mg}(\text{OH})_2$  slurry carbonation. *Ind. Eng. Chem. Res.* **53**, 18170–18179 (2014).
137. Stack, A. G. et al. Pore-size-dependent calcium carbonate precipitation controlled by surface chemistry. *Environ. Sci. Technol.* **48**, 6177–6183 (2014).
138. Ilavsky, J. et al. Development of combined microstructure and structure characterization facility for in situ and operando studies at the Advanced Photon Source. *J. Appl. Crystallogr.* **51**, 867–882 (2018).
139. Gadikota, G., Zhang, F. & Allen, A. In situ angstrom-to-micrometer characterization of the structural and microstructural changes in kaolinite on heating using ultrasmall-angle, small-angle, and wide-angle X-ray scattering (USAXS/SAXS/WAXS). *Ind. Eng. Chem. Res.* **56**, 11791–11801 (2017).
140. Gadikota, G. & Allen, A. in *Materials and Processes for  $\text{CO}_2$  Capture, Conversion, and Sequestration* (eds Li, L., Wong-Ng, W., Huang, K. & Cook, L. P.) 296–318 (Wiley, 2018).
141. Gadikota, G. Connecting the morphological and crystal structural changes during the conversion of lithium hydroxide monohydrate to lithium carbonate using multi-scale X-ray scattering measurements. *Minerals* **7**, 169 (2017).
142. Yang, Z.-Z., Zhao, Y.-N. & He, L.-N.  $\text{CO}_2$  chemistry: task-specific ionic liquids for  $\text{CO}_2$  capture/activation and subsequent conversion. *RSC Adv.* **1**, 545–567 (2011).
143. Yang, Z.-Z. et al.  $\text{CO}_2$  capture and activation by superbase/polyethylene glycol and its subsequent conversion. *Energy Environ. Sci.* **4**, 3971–3975 (2011).
144. Liu, A.-H. et al. Equimolar  $\text{CO}_2$  capture by N-substituted amino acid salts and subsequent conversion. *Angew. Chem. Int. Ed.* **51**, 11306–11310 (2012).
145. Jiang, B. et al. Development of amino acid and amino acid-complex based solid sorbents for  $\text{CO}_2$  capture. *Appl. Energy* **109**, 112–118 (2013).
146. Feron, P. H. M. & ten Asbroek, N. in *Greenhouse Gas Control Technologies 7* Vol. 2 (eds Rubin, E. S. et al.) 1153–1158 (Elsevier, 2005).
147. Huang, Q., Bhatnagar, S., Remias, J. E., Selegue, J. P. & Liu, K. Thermal degradation of amino acid salts in  $\text{CO}_2$  capture. *Int. J. Greenh. Gas Control* **19**, 243–250 (2013).

## Acknowledgements

This research was supported by the US Department of Energy, Office of Science, Basic Energy Sciences, Chemical Sciences, Geosciences, and Biosciences Division.

## Competing interests

Provisional patents have been filed by Cornell University on the process for directed hydrogen synthesis starting with calcium and magnesium silicate precursors and the reactive separation of  $\text{CO}_2$  using amine-bearing solvents.

## Publisher's note

Springer Nature remains neutral with regard to jurisdictional claims in published maps and institutional affiliations.

© Springer Nature Limited 2020